Geoderma 453 (2025) 117159

Contents lists available at ScienceDirect

Geoderma

journal homepage: www.elsevier.com/locate/geoderma

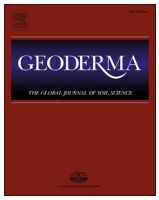

Nitrogen input decreases microbial nitrogen use efficiency in surface soils of a temperate forest in northeast China

Lifei Sun [a], Yanci Qiao [a], Wolfgang Wanek [c], Daryl L. Moorhead [d], Yongxing Cui [e], Yujiao Peng [a], Liquan Song [a], Baoqing Hu [a], Tuo Zhang [a], Shuailin Li [b,*]

[a] Key Laboratory of Environment Change and Resources Use in Beibu Gulf, Ministry of Education, and Guangxi Key Laboratory of Earth Surface Processes and Intelligent Simulation of Nanning Normal University, Nanning 530001, China
[b] Institute of Applied Ecology, Chinese Academy of Sciences, 110016 Shenyang, China
[c] Division of Terrestrial Ecosystem Research, Center of Microbiology and Environmental Systems Science, University of Vienna, Djerassiplatz 1, 1030 Vienna, Austria
[d] Department of Environmental Sciences, University of Toledo, 43606, Toledo, USA
[e] Institute of Biology, Freie Universität Berlin, Berlin, Germany

ARTICLE INFO

Handling Editor: D. Said-Pullicino

Keywords:
Microbial growth
soil N transformation
soil C storage
Global change
Soil depth
Nutrient limitation

ABSTRACT

Microbial nitrogen use efficiency (NUE) reflects the allocation of microbially-acquired N between growth (anabolism) and the release of inorganic N to the environment (catabolism), and is central to understanding soil N cycling. However, the effects of N addition on microbial NUE are unclear. We determined microbial NUE in surface (0–10 cm) and subsurface (10–20 cm) soils in a temperate forest by the combined substrate-independent ^{18}O-H_2O tracer technique and ^{15}N isotope pool dilution in a multi-level N addition experiment. We found that high N treatment (75 kg N ha^{-1} yr^{-1} as urea fertilizer) significantly decreased NUE in surface soil, but not in the subsurface soil. The decrease in NUE in surface soil was related to soil acidification, likely induced by N addition, and to reduced phosphorus availability, suggesting increased phosphorus limitation to microbial metabolism with N addition. Microbial NUE was inversely related to inorganic N flux (as NH_4^+) in both surface and subsurface soils and positively related to microbial biomass in surface soil. Our empirical evidence confirms that microbial NUE is a sensitive proxy and controlling branchpoint between soil microbial N immobilization and inorganic N cycling, which should be explicitly included in biogeochemical models to better predict soil N dynamics.

1. Introduction

Nitrogen-containing compounds in soils primarily exist in the form of polymers that can be utilized by plants and microbes after they are depolymerized and released as low-molecular-weight compounds (such as amino acids and nucleotides) by extracellular enzymes (Jan et al., 2009; Schimel and Bennett, 2004). Microbes use this organic N for biomass synthesis (or growth) and excrete the excess N in the form of inorganic N (mainly as NH_4^+-N; gross N mineralization) (Schimel and Bennett, 2004). Microbial nitrogen use efficiency (NUE) indicates the partitioning of the acquired organic N between biomass synthesis and NH_4^+-N production (Mooshammer et al., 2014a). Therefore, microbial NUE quantifies the conversion of organic N to inorganic N with significant implications for soil N availability, N transformation processes, risk of N loss, and primary production of ecosystems (Sun et al., 2023a; Zhang et al., 2019).

Over the past decades, atmospheric N deposition rates in large regions of the world have greatly increased compared with rates in the preindustrial era, due to increased anthropogenic activities such as agricultural intensification, industrial and urban development, and fuel usage (Dentener et al., 2006; Galloway et al., 2008). The N deposition level is predicted to double by 2050 with some regions exceeding 50 kg N ha^{-1} yr^{-1} (Galloway et al., 2008). China is one of three regions that exhibit among the highest N deposition fluxes in the world. The average N deposition rate in China is 20.4 kg N ha^{-1} yr^{-1} and the highest rates exceed 50 kg N ha^{-1} yr^{-1} in North China (Yu et al., 2019). Increased reactive N input has strong impacts on soil microbial physiology, biogeochemical cycling, and the stability of forest ecosystems (Li et al., 2021; Zhu et al., 2015). Clarifying the effects of N enrichment on microbial NUE and its underlying mechanisms is important for understanding the response and feedback of N cycling in forest ecosystems.

Microbial NUE could be affected by atmospheric N deposition

* Corresponding author.
E-mail address: lishuailin007@163.com (S. Li).

https://doi.org/10.1016/j.geoderma.2024.117159
Received 20 July 2024; Received in revised form 19 December 2024; Accepted 23 December 2024
Available online 25 December 2024

through multiple mechanisms. When microbes are strongly limited by N, microbial NUE should be at its maximum according to predictions of stoichiometric homeostasis, with N being preferentially allocated towards biosynthesis and growth (Mooshammer et al., 2014a). Accordingly, increasing N availability may decrease microbial NUE, due to decreasing allocation of N to growth but increasing partitioning of N to catabolism and mineralization. Also, increased N inputs may acidify the soil, which in turn inhibits microbial growth and therefore decreases microbial NUE (Sun et al., 2023a). Previous studies found elevated N inputs to induce phosphorus (P) limitation in tropical forests where P availability is low (Deng et al., 2017). Although temperate forests are often considered to be N-limited this is not always true (Cui et al., 2021) and long-term N input may exacerbate P limitations, affecting microbial N metabolism (Mooshammer et al., 2014a; Sun et al., 2023a). Finally, changes in microbial community composition and diversity under elevated N input may also affect microbial NUE because growth rate and metabolic efficiency vary among microbial taxa (Mooshammer et al., 2014b; Pold et al., 2020; Zhang et al., 2018).

Soil characteristics, such as organic carbon content, pH, nutrient availability, and soil texture, typically vary with soil depth, which can affect the responses of microbial NUE to N input (Li et al., 2021). Additionally, the retention of N in surface soils and plant uptake can reduce the amount of exogenous N entering subsurface soils, resulting in different NUE responses to N input at varying soil depths (Liu et al., 2017). Seasonal changes in environmental conditions and plant growth may also affect microbial NUE and its response to N input by influencing soil temperature and substrate availability, respectively (Mooshammer et al., 2014b; Zhang et al., 2019). However, few studies have examined the interactions between N input, season, and soil depth with respect to microbial NUE, which limits our ability to predict soil N dynamics under future environmental changes.

Microbial NUE is an important metric of soil N cycling (Zhang et al., 2019), but soil N transformation processes are complex and sensitively respond to substrate concentration (Müller et al., 2007; Sun et al., 2019; Zhang et al., 2011) and environmental factors (Elrys et al., 2021a; Elrys et al., 2021b). However, little is known whether and to which extent anabolic and catabolic N processes respond differently to environmental factors, thereby altering NUE and inorganic N cycling (Zhang et al., 2019). Changes in soil microbial NUE likely have strong downstream effects, for instance an increased NH_4^+-N release, which reflects reduced NUE, may stimulate NH_4^+-N consumption processes (e.g. nitrification, anaerobic ammonia oxidation, nitrification-derived N_2O production, and ammonium sorption), and in turn the NO_3^--N produced by nitrification may stimulate NO_3^--N consumption processes (e.g. denitrification, nitrate leaching, and dissimilatory nitrate reduction to ammonium) (Sun et al., 2019; Zhang et al., 2011; Zhang et al., 2019). The gross N mineralization process is considered to be the main factor determining soil inorganic N availability in natural ecosystems (Li et al., 2020), therefore microbial NUE is closely related to the entire soil inorganic N cycle through gross N mineralization. In contrast, high microbial NUE indicates reduced N mineralization with relatively more N used for biosynthesis, contributing to biomass production and soil N retention (Sun et al., 2023b). Hence, microbial NUE may exhibit a positive relationship with microbial biomass and a negative relationship with inorganic N flux. Increased N inputs may affect microbial biomass and soil inorganic N cycling by affecting microbial NUE.

Based on a long-term N addition experiment in a temperate forest in Northeastern China, we investigated the effects of N enrichment on microbial NUE and explored the relationship between microbial NUE, microbial biomass and soil inorganic N cycling. We hypothesized that (1) N input decreases NUE in surface soil due to soil acidification impairing microbial N assimilation and growth, but has no such effect in subsurface soil due to the buffering effect of surface soil; (2) seasonal changes influence NUE by affecting soil temperature and substrate availability; and (3) microbial NUE is positively related to microbial biomass and negatively related to soil inorganic N cycling activity, because microbial NUE controls the balance between anabolic (biomass N synthesis) and catabolic (NH_4^+-N release) N processes.

2. Material and methods

2.1. Experimental design and soil sample collection

The experimental area is located in the Changbai Mountain Natural Nature Reserve in Jilin Province, Northeastern China (42.70 °N, 127.63 °E). This region is characterized by a typical temperate climate, with long, cold winters and warm summers. The mean annual temperature is about 4 °C, with the highest temperature occurring in July and the lowest in January. The mean annual precipitation is 745 mm. The soil is a dark brown soil (Albic Luvisol) developed from volcanic ash (Bai et al., 2014). We established an N addition experiment in a Korean pine and broadleaf mixed forest in 2014, which consists of twelve experimental plots (50 × 50 m), the buffer zones between plots being at least 20 m. The N addition experiment had four levels (three replicates per level): control (0 kg N ha^{-1} yr^{-1}), low N levels (25 kg N ha^{-1} yr^{-1}), medium N levels (50 kg N ha^{-1} yr^{-1}), and high N levels (75 kg N ha^{-1} yr^{-1}). Urea was spread as slow release N fertilizer. The atmospheric N deposition rate in this area is about 27 kg N ha^{-1} yr^{-1}, therefore the amount of N added at medium N and high N levels is equivalent to about two times and three times the ambient N deposition rate, respectively (Sun et al., 2023b). Detailed information for the fertilizer experiment is in Li et al. (2021).

We sampled soils in June, July, August, September, and October of 2021 (8 years after treatment) and measured soil temperature using a PT100 thermometer during each sampling campaign. In each plot, fifteen subsamples were collected with an auger (5 cm diameter) from both surface (0–10 cm) and subsurface soils (10–20 cm) after removing the surface plant litter. These subsamples were mixed to form a composite sample for each soil horizon and transported to the laboratory. Each composite sample was divided into three subsamples after sieving (2 mm) and then stored at 4 °C, −20 °C, or air-dried, for analyses of microbial NUE, enzyme activity, and soil properties, respectively. Soil properties (organic carbon, total nitrogen, clay, silt, sand, and bulk density) were only determined once because we assumed that these characteristics did not change markedly during one season.

2.2. Soil N transformation rates

Laboratory incubation experiments were set up to determine N transformation rates, microbial growth, and NUE. For each composite soil, we prepared five conical flasks containing 20 g fresh soil (oven-dry base), with four for soil N transformation rate determination and one for microbial growth determination. Soil moisture was set to 60 % water holding capacity and then preincubated for 24 h at the *in situ* soil temperature of the collection month. Soil temperatures in June, July, August, September, and October were 16 °C, 21 °C, 18 °C, 11 °C, and 7 °C. Gross N transformation rates were evaluated with ^{15}N isotope pool dilution techniques, with the addition of ^{15}N enriched ammonium ($^{15}NH_4NO_3$) and ^{15}N enriched nitrate ($NH_4^{15}NO_3$) as tracers. After preincubation, two flasks were amended with $NH_4^{15}NO_3$ and the other two were amended with $^{15}NH_4NO_3$. Aliquots of 1 ml $^{15}NH_4NO_3$ or $NH_4^{15}NO_3$ (at 10 atom% ^{15}N) solution were added to each conical flask at a rate of 20 μg N g^{-1} soil as NH_4^+-N or NO_3^--N. Then, these conical flasks were incubated at the respective *in situ* soil temperatures for 0.5 h and 48 h. Solutions of 2 M KCl (1:5(w:v)) were used to extract NH_4^+-N and NO_3^--N after incubation. The concentrations of NH_4^+-N and NO_3^--N in extracts were analyzed with a continuous-flow analyzer (Skalar Analytical, Breda, The Netherlands). The ^{15}N abundances of NH_4^+-N and NO_3^--N in extracts were determined by the microdiffusion method (Brooks et al., 1989). Both NH_4^+-N and NO_3^--N were collected for ^{15}N abundance determinations by sequentially adding MgO and Devarda's alloy. Acidified glass fiber disks were used to trap the liberated NH_3. The ^{15}N

abundances of NH_4^+-N and NO_3^--N were measured by an Isotope Ratio Mass Spectrometer (Thermo Fisher MAT 253, USA).

2.3. Microbial growth and NUE

Microbial growth and NUE were evaluated by the ^{18}O-H_2O tracer technique (Zhang et al., 2019). For each composite soil, two brown chromatographic vials (2 ml) were prepared, each containing 1 g of soil from the remaining conical flask. The ^{18}O-H_2O (98 atom%) was added to one vial to achieve a final ^{18}O enrichment of 20 atom% in soil water and the other vial received an equal volume of water at natural abundance as a control. Then, the vials were incubated for 48 h at the *in situ* soil temperature. After incubation, vials were stored at −20 °C for ^{18}O abundance analysis of DNA. The remaining pre-incubated soil in each conical flask was used for analysis of microbial biomass (see section 2.4). We used the DNeasy PowerSoil Kit (Qiagen, Hilden, Germany) to extract total DNA in ^{18}O-labeled and non-labeled soils. We used a multi-functional microplate reader (Synergy^{H4} Hybrid Reader, Synergy^{H4} BioTek, USA) to estimate DNA quantity. Then, aliquots (70 μl) of the DNA solutions were added to silver capsules and dried at 45 °C. The abundance and concentration of O derived from the DNA were measured with a TC/EA-IRMS system (Thermo Scientific, USA). The remaining DNA was used for amplicon sequencing. The primer sets ITS1F/ITS2 and 515F/806R were used to amplify the fungal ITS gene and the V4 region of the bacterial 16 s rRNA gene, respectively. Details of experimental processes and data analyses can be found in Sun et al. (2023a). We conducted non-metric multidimensional scaling (NMDS) analysis based on Bray-Curtis distance to describe bacterial and fungal community composition (Domeignoz-Horta et al., 2020; Yang et al., 2022). The sequencing dataset have been deposited to figshare database with a doi number: https://doi.org/10.6084/m9.figshare.25515166.

2.4. Soil properties

Soil pH was assayed in a water-to-soil ratio of 2.5:1 (v:w) using a pH meter. Soil organic carbon, soil total N, and soil C/N were determined using an elemental analyzer (Vario MACRO cube, Germany). The chloroform fumigation method was used to determine microbial biomass C (MBC), microbial biomass N (MBN), and microbial biomass P (MBP) (Brookes et al., 1982; Vance et al., 1987). Briefly, two conical flasks, each containing 5 g of soil from the composite sample, were prepared. One flask was fumigated for 48 h with $CHCl_3$ and then extracted with 20 ml of 0.5 M K_2SO_4, while the other flask was extracted with K_2SO_4 without $CHCl_3$ fumigation. The C, N, and P contents in the non-fumigated extractions were used to indicate dissolved organic C (DOC), dissolved nitrogen (DN), and dissolved P (DP), respectively (Li et al., 2021; Sang et al., 2021). Microbial biomass C, N, and P were calculated as the differences in DOC, DN, and DP in extracts between non-fumigated and fumigated subsamples. The pipette-sedimentation method was used to estimate soil texture (Gee and Bauder, 1986). The contents of mineral-associated organic matter (MAOM) and particulate organic matter (POM) were determined by a size fractionation procedure (Poeplau et al., 2018). Briefly, soil samples were shaken in sodium hexametaphosphate solution for 18 h and then rinsed through a 53 μm sieve. The soil fraction retained in the sieve was considered to be POM and the soil fraction passing through (<53 μm) was considered to represent MAOM. The C and N contents of POM and MAOM were analyzed with the elemental analyzer (Vario MACRO cube, Germany).

2.5. Extracellular enzyme activity

The extracellular enzyme activities of leucine aminopeptidase (LAP), β-1,4-N-acetylglucosaminidase (NAG), acid phosphatase (AP), and β-1,4-glucosidase (BG) were determined according to Saiya-Cork et al. (2002), following modifications by German et al. (2011) and Allison et al. (2009). Briefly, 1 g of soil sample was added to 125 ml of acetate buffer (50 mM, pH 5.0), and the sample suspension was blended for 1 min. Then, 200 μl of sample suspension and 50 μl of 200 μM substrate solution were dispensed into the sample wells of 96-well microplates. In the blank wells, 200 μl of sample suspension and 50 μl of acetate buffer were dispensed. In the negative control wells, 200 μl of acetate buffer and 50 μl of substrate solution were dispensed. Quench standard wells received 200 μl of sample suspension and 50 μl of standard solution (10 μM 4 methylumbelliferone, or 7-amino-4-methyl coumarin in the case of LAP analysis). Reference standard wells received 50 μl of standard solution and 200 μl acetate buffer. The microplates were incubated in the dark for 4 h at 20 °C. Fluorescence was evaluated by a multi-functional microplate reader with 450 nm emission and 365 nm excitation filters.

2.6. Phospholipid fatty acid (PLFA) analysis

Lipid extractions and PLFA analyses were performed as described by Wang et al. (2014). Briefly, freeze-dried soil (5 g) was extracted with chloroform/methanol/phosphate buffer mixture (1:2:0.8, 0.15 M, pH 4.0). Phospholipids were separated from neutral lipids and glycolipids using silicic acid columns and fractional elution. The gas chromatograph (GC 7890A; Agilent, Santa Clara, CA, USA) and the MIDI Sherlock microbial identification system were used for the identification and annotation of the resultant fatty acid methyl esters, respectively. PLFA biomarkers were grouped into different microbial origins based on previous studies (Francisco et al., 2022; Frostegård et al., 1993; Olsson et al., 1999). The abundance of total PLFAs was the sum of all detected fatty acids and was used to indicate living soil microbial biomass.

2.7. Calculations

Soil gross N mineralization (also called gross NH_4^+-N production or gross ammonification) and gross nitrification (also called gross NO_3^--N production) rates were estimated according to Kirkham and Bartholomew (1954). Specifically, gross N mineralization (GNM) rates (ng N g^{-1} soil h^{-1}) were calculated as follows:

$$GNM = \frac{C_{t2} - C_{t1}}{t_2 - t_1} \times \frac{ln(APE_{t1}/APE_{t2})}{ln(C_{t2}/C_{t1})} \quad (1)$$

where APE is ^{15}N atom% excess of NH_4^+-N, t_2 and t_1 refer to incubation stop time (h), and C_{t2} and C_{t1} refer to soil NH_4^+-N concentrations (ng N g^{-1} soil) at t_2 and t_1, repectively. Gross nitrification rates (GN, ng N g^{-1} soil h^{-1}) were estimated by replacing NH_4^+-N atom% excess and NH_4^+-N concentration in equation (1) with NO_3^--N atom% excess and NO_3^--N concentration.

Both, gross NH_4^+-N and NO_3^--N consumption rates were evaluated as the difference between net and gross rates (Huygens et al., 2008). Specifically, NH_4^+-N consumption (C_{NH4}, ng N g^{-1} soil h^{-1}), which refers to the sum of all potential consumption processes of ammonium (e.g. the processes of nitrification, nitrification-derived N_2O and NO production, and mineral immobilization), was calculated as:

$$C_{NH4} = GNM - \frac{(C_{t2} - C_{t1})}{(t_2 - t_1)} \quad (2)$$

Gross NO_3^--N consumption (C_{NO3}, ng N g^{-1} soil h^{-1}), which refers to the sum of all potential consumption processes of nitrate (e.g. process of assimilatory and dissimilatory NO_3^--N metabolism, including denitrification-derived N_2, N_2O, and NO production), was calculated by replacing GNM and NH_4^+-N concentrations in equation (2) with gross nitrification rates and NO_3^--N concentrations.

Because NH_4^+-N production by gross N mineralization provides the substrate for gross nitrification, gross N mineralization can stimulate gross nitrification. Meanwhile, consumption processes of NH_4^+-N and NO_3^--N can also be stimulated by increased gross N mineralization and gross nitrification, respectively. Therefore, the activity of the soil inorganic N cycle can be formulated as a new metric, i.e., the soil inorganic N

cycling flux (NCF, ng N g^{-1} soil h^{-1}), which is calculated as the sum of GNM, C_{NH4}, and C_{NO3}. Gross nitrification rates were not included in the NCF estimates, because C_{NH4} includes the gross nitrification process (Davidson et al., 1991).

The amount of DNA produced ($DNA_{produced}$, ng) over a 48-hour incubation period was determined according to Zhang et al. (2019):

$$DNA_{produced} = O_{total} \times \frac{at\%_{excess}}{100} \times \frac{100}{at\%_{label}} \times \frac{100}{31.21} \quad (3)$$

where 31.21 refers to the average weight% of O in DNA ($C_{32}H_{44}O_{24}N_{15}P_4$), O_{total} indicates the O content in the dried DNA (ng), and $at\%_{excess}$ indicates the difference in atom% of ^{18}O between labeled and unlabeled samples.

Microbial N growth rate (N_{growth}, ng N g^{-1} soil h^{-1}) was estimated as:

$$N_{growth} = \frac{DNA_{produced} \times f_{DNA}}{t \times DW} \quad (4)$$

where DW and t refer to soil dry mass (g) and incubation time (h), respectively. The f_{DNA} (unitless) indicates the ratio of MBN (ng g^{-1} soil) to soil DNA content (ng g^{-1} soil).

Microbial NUE was calculated as:

$$NUE = \frac{N_{growth}}{N_{growth} + GNM} \quad (5)$$

2.8. Statistical analyses

The effects of N treatment, sampling time (month), soil horizon, and their interactions on measured variables were estimated with the linear mixed-effect models with plot as random effect using the "nlme" package (Pinheiro, 2011). The Tukey test was applied for post hoc multiple comparisons. Negative NUE values were observed in October in the subsurface soils likely due to the inhibition of microbial growth at low temperature. These negative values were removed from analyses (Domeignoz-Horta et al., 2020). The type III sums of squares were used to correct for the unbalanced design. Prior to statistical analysis, data were transformed to improve variance homogeneity if necessary. Pearson correlation analysis was performed to assess the relationships between measured variables with the "corrplot" package (Wei et al., 2017). The bivariate relationships between NUE and measured variables (soil properties, environmental variables, and microbial variables) were explored using linear mixed-effects models with plot as the random effect (Fig. 2). Random forest analysis was conducted to estimate important predictors of NUE, total PLFA, and NCF using the "rfPermute" package (Archer, 2016). Stepwise multiple linear regression was used to explore the relationships between NUE and total PLFA and NCF. Piecewise structural equation models (SEM) were used to assess direct and indirect effects among variables under N input. The conceptual SEM model was established based on our working hypothesis and the findings from correlation analysis and stepwise regression analysis. The SEM analysis considered the random effect of plot and modeled the correlation among sampling months with a continuous autoregressive 1 autocorrelation structure. Fisher's C was used as the goodness-of-fit statistic and $P > 0.05$ indicates a well-fit model. The SEM was conducted using the "piecewiseSEM" package (Lefcheck, 2016). The least significant paths were removed stepwise to improve parsimoniousness of the SEM and the optimum model was selected by comparing Akaike information criterion values among nested models (Shipley, 2013). Because microbial NUE is calculated from gross N mineralization rates and microbial growth rates (Eq. (5), the latter two parameters were not included in random forest analysis and in SEM analysis (Fig. S8), consistent with previous studies (Domeignoz-Horta et al., 2020; Malik et al., 2018; Spohn et al., 2016). All statistical analyses were conducted in R 4.1.2 (Lever et al., 2015) and figures were made in R using the "ggplot2" package (Valero-Mora, 2010).

3. Results

3.1. Effects of N addition on soil properties and microbial NUE

No significant changes in SOC, TN, soil C/N, BD, and fractions of clay, silt, and sand were detected after N addition in either surface or subsurface soils (Table 1). However, SOC, TN, soil C/N, and the sand fraction were significantly higher in the surface soil than in the subsurface soil whereas soil clay, silt, and BD were lower in the surface soil.

In general, high N addition tended to decrease both NUE and microbial N growth rates in the surface soil compared to the control group (CK) across all monthly samplings (Table S1 and Fig. 1 and S1), however, it did not impact gross N mineralization rates. In the subsurface soil, N addition did not affect NUE, microbial N growth rates or gross N mineralization rates. Gross N mineralization rates and microbial N growth rates were significantly higher in the surface soil than in the

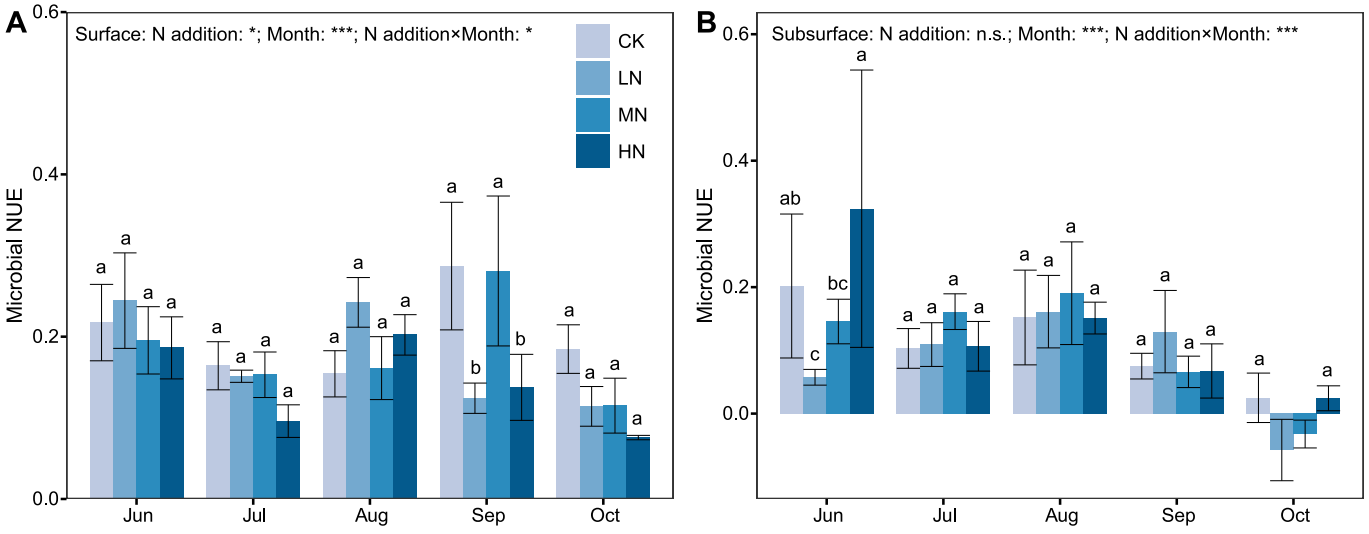

Fig. 1. Effects of N addition on microbial nitrogen use efficiency (NUE) in surface (A) and subsurface (B) soils. CK, control (0 kg N^{-1} ha^{-1} yr^{-1}); LN, low N addition (25 kg N^{-1} ha^{-1} yr^{-1}); MN, medium N addition (50 kg N^{-1} ha^{-1} yr^{-1}); HN, high N addition (75 kg N^{-1} ha^{-1} yr^{-1}). The effects of treatment (N addition), sampling time (Month), and their interaction (N addition × Month) in each soil horizon are shown. *, $P < 0.05$; **, $P < 0.01$; ***, $P < 0.001$. Different lower-case letters indicate a significant difference among N addition treatments in a specific month. Data presented are means and standard errors ($n = 3$).

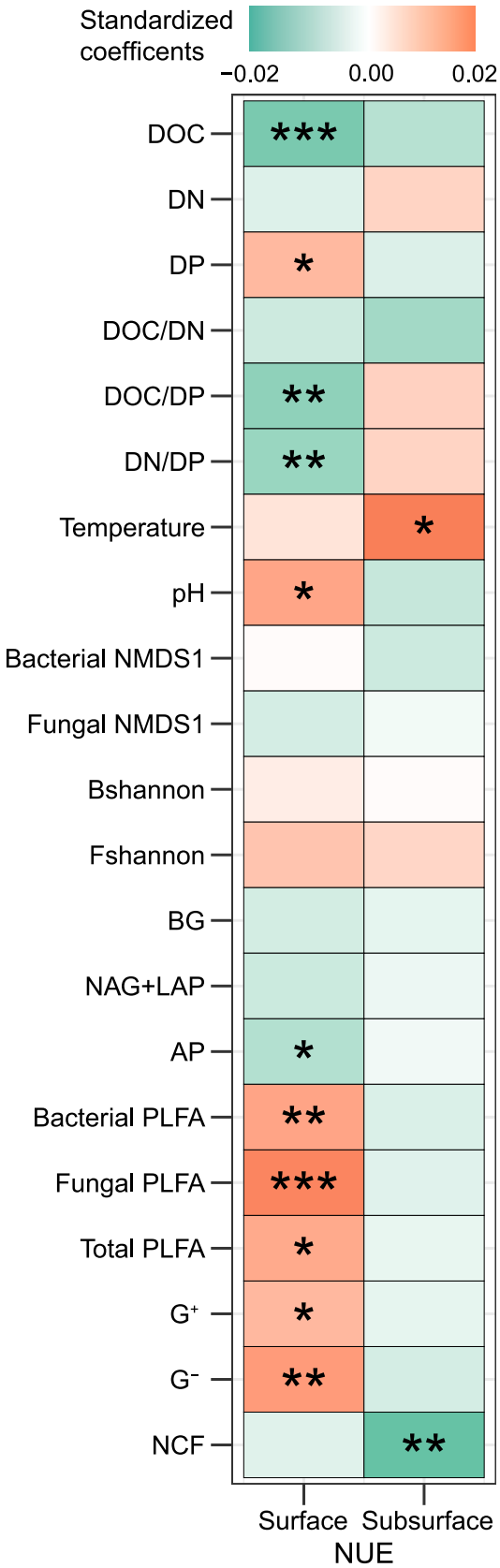

(caption on next column)

Fig. 2. The bivariate relationships between measured variables and microbial NUE in surface and subsurface soils. DOC, dissolved organic carbon (μg g^{-1}); DN, dissolved nitrogen (μg g^{-1}); DP, dissolved phosphorus (μg g^{-1}); DOC/DN, the ratio of dissolved organic carbon to dissolved nitrogen; DOC/DP, the ratio of dissolved organic carbon to dissolved phosphorus; DN/DP, the ratio of dissolved nitrogen to dissolved phosphorus. Bacterial NMDS1, bacterial community non-metric multidimensional scaling (NMDS) axis 1; fungal NMDS1, fungal community non-metric multidimensional scaling (NMDS) axis 1; Bshannon, bacterial Shannon index; Fshannon, fungal Shannon index; BG, β-1,4-glucosidase (nmol h^{-1} $nmol^{-1}$ PLFA); NAG, β-1,4-N-acetylglucosaminidase (nmol h^{-1} $nmol^{-1}$ PLFA); LAP, leucine aminopeptidase (nmol h^{-1} $nmol^{-1}$ PLFA); AP, acid phosphatases (nmol h^{-1} $nmol^{-1}$ PLFA); PLFA, phospholipid fatty acids (nmol g^{-1}); G^+, gram-positive bacteria (nmol g^{-1}); G^-, gram-negative bacteria (nmol g^{-1}); NCF, composite inorganic nitrogen cycling flux (ng g^{-1} h^{-1}). The data was standardized before analysis. *, $P < 0.05$, **, $P < 0.01$, ***, $P < 0.001$.

subsurface soil, however, there was no significant difference in NUE between both soil layers (Table S1). Compared to CK, high N addition resulted in a small but consistent decrease in soil pH, i.e. by 0.25 units in surface soil and by 0.14 units in subsurface soil (Fig. S1). Soil pH and the fraction of mineral-associated organic matter in the subsurface soil were significantly higher than in the surface soil (Table S1 and Fig. S1 and S3). The DOC content was significantly higher in October than in the other months in both surface and subsurface soils (Fig. S2).

3.2. Relationships between measured variables

Microbial NUE was positively related to microbial N growth rates and negatively related to gross N mineralization rates in both surface and subsurface soils (Fig. S4 and equation (5). In surface soil, NUE was positively related to DP, soil pH, bacterial PLFA, fungal PLFA, total PLFA, gram-positive bacteria (G^+), and gram-negative bacteria (G^-), and negatively related to DOC, DOC/DP, DN/DP, and acid phosphatases (AP) activity (Fig. 2). In subsurface soil, NUE was positively related to temperature because increasing temperature stimulated microbial N growth rates but did not affect gross N mineralization (Fig. 2 and S5). In surface soil, temperature was positively related to both microbial N growth rates and gross N mineralization rates but showed no relationship with NUE (Fig. 2 and S5).

Total PLFA, fungal PLFA, and bacterial PLFA were negatively related to DOC, DOC/DN, and DOC/DP, and positively related to DP, temperature, microbial N growth rate, and NCF in surface soil (Fig. S5). In subsurface soil, total PLFA, fungal PLFA, and bacterial PLFA were positively related to DN and negatively related to extracellular enzyme activities (BG, NAG + LAP, and AP). Fungal PLFA was negatively related to the N addition rate in the surface soil but showed no relationship in the subsurface soil. DOC was negatively related to DP in both surface and subsurface soils. Soil pH and DP were positively related to microbial N growth rate in the surface soil but showed no relationships in the subsurface soil (Fig. S5).

The random forest analyses indicated that DOC/DP, soil pH, DOC, temperature, DN/DP, DP, and N addition treatment were significant predictors for NUE in surface soil, but only temperature was a significant predictor for NUE in subsurface soil (Fig. 3).

3.3. Effects of microbial NUE on microbial biomass and soil inorganic N cycling

Random forest analysis indicated that temperature, bacterial community composition, NUE, DOC/DN, and DOC were significant predictors for total PLFA in surface soil, and subsequent stepwise regression analysis retained temperature, microbial NUE, and bacterial community structure in the final model, with a positive effect of NUE on total PLFA (Fig. 3 and Table S2). In subsurface soil, the random forest analysis indicated that DOC/DN, DN, and N addition treatment but not NUE were significant predictors for total PLFA.

Table 1
Effects of N addition on soil properties.

Soil horizon	Treatment	SOC (%)	TN (%)	C/N	Clay (%)	Silt (%)	Sand (%)	BD (g cm^{-3})
Surface	CK	11.15 ± 0.40 a	0.89 ± 0.08 a	12.61 ± 0.73 a	30.76 ± 1.36 a	35.13 ± 1.76 a	34.12 ± 2.94 a	0.49 ± 0.05 a
(0–10 cm)	LN	9.89 ± 1.12 a	0.82 ± 0.09 a	12.11 ± 0.76 a	29.29 ± 2.81 a	35.77 ± 1.55 a	34.94 ± 3.88 a	0.51 ± 0.06 a
	MN	10.98 ± 0.73 a	0.93 ± 0.09 a	11.77 ± 0.36 a	32.16 ± 2.75 a	36.73 ± 2.29 a	31.11 ± 4.12 a	0.45 ± 0.07 a
	HN	9.63 ± 0.50 a	0.83 ± 0.01 a	11.61 ± 0.78 a	28.80 ± 6.74 a	35.02 ± 2.61 a	36.18 ± 9.34 a	0.51 ± 0.03 a
Subsurface	CK	2.37 ± 0.46 a	0.23 ± 0.04 a	10.41 ± 0.10 a	37.67 ± 3.83 a	42.98 ± 0.48 a	19.35 ± 4.19 a	0.76 ± 0.04 a
(10–20 cm)	LN	2.99 ± 0.47 a	0.29 ± 0.05 a	10.46 ± 0.03 a	38.26 ± 0.49 a	41.82 ± 1.18 a	19.92 ± 1.59 a	0.83 ± 0.01 a
	MN	2.65 ± 0.75 a	0.24 ± 0.08 a	10.30 ± 0.16 a	34.59 ± 6.01 a	38.67 ± 5.69 a	26.74 ± 11.42 a	0.71 ± 0.04 a
	HN	2.47 ± 0.83 a	0.30 ± 0.06 a	10.25 ± 0.17 a	37.24 ± 0.82 a	42.30 ± 1.73 a	20.46 ± 2.55 a	0.70 ± 0.13 a
ANOVA results								
N addition		n.s.	n.s.	n.s.	n.s.	n.s.	n.s.	n.s.
Horizon		***	***	***	***	***	***	***
N addition × Horizon		*	n.s.	n.s.	n.s.	n.s.	n.s.	n.s.

CK, control (0 kg N^{-1} ha^{-1} yr^{-1}); LN, low N addition (25 kg N^{-1} ha^{-1} yr^{-1}); MN, medium N addition (50 kg N^{-1} ha^{-1} yr^{-1}); HN, high N addition (75 kg N^{-1} ha^{-1} yr^{-1}). *, $P < 0.05$; **, $P < 0.01$; ***, $P < 0.001$. Different lower-case letters indicate a significant difference among N addition treatments in a specific soil horizon. Data presented are mean and standard error ($n = 3$). SOC, soil organic carbon; TN, total nitrogen; C/N, SOC/TN; BD, bulk density.

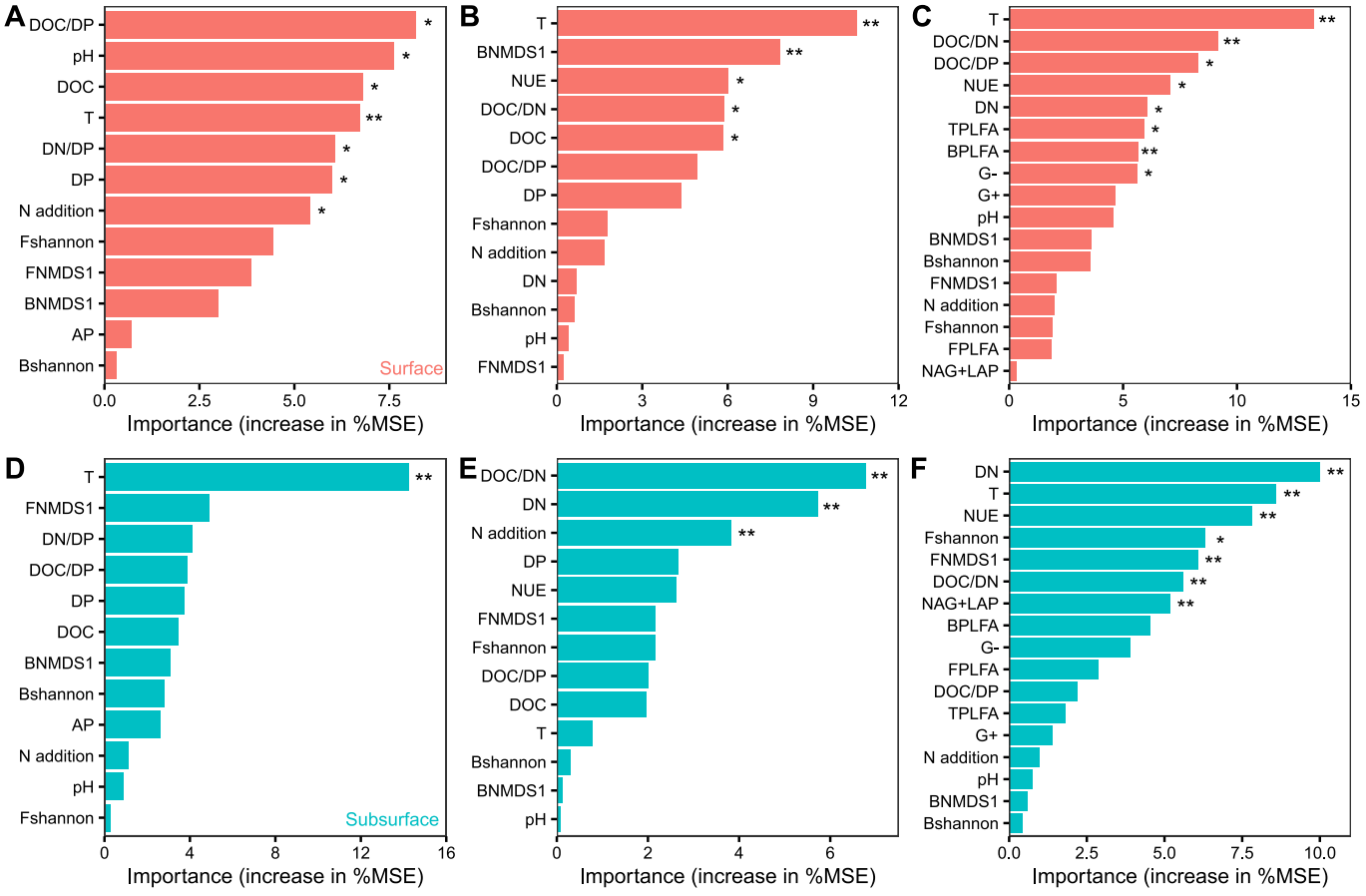

Fig. 3. Importance of predictors for microbial NUE (A, D), total PLFA (B, E), and NCF (C, F) in surface and subsurface soils based on the random forest analyses. MSE, mean square error; DOC, dissolved organic carbon (μg g^{-1}); DN, dissolved nitrogen (μg g^{-1}); DP, dissolved phosphorus (μg g^{-1}); DOC/DN, the ratio of dissolved organic carbon to dissolved nitrogen; DOC/DP, the ratio of dissolved organic carbon to dissolved phosphorus; DN/DP, the ratio of dissolved nitrogen to dissolved phosphorus; AP, acid phosphatases (nmol h^{-1} $nmol^{-1}$ PLFA); BNMDS1, bacterial community non-metric multidimensional scaling (NMDS) axis 1; Bshannon, bacterial Shannon index; FNMDS1, fungal community non-metric multidimensional scaling (NMDS) axis 1; Fshannon, fungal Shannon index; PLFA, phospholipid fatty acid (nmol g^{-1}); T, temperature (°C); NUE, nitrogen use efficiency; NCF, composite inorganic nitrogen cycling flux (ng g^{-1} h^{-1}). *, $P < 0.05$, **, $P < 0.01$.

Moreover, random forest analysis indicated that temperature, DOC/DN, DOC/DP, NUE, DN, total PLFA, bacterial PLFA, and gram-negative bacteria were significant predictors for NCF in the surface soil, and subsequent stepwise regression analysis retained temperature, total PLFA, and NUE in the final model, with a negative effect of NUE on NCF (Fig. 3 and Table S2). In subsurface soil, the random forest analysis indicated that DN, temperature, NUE, fungal diversity and community composition, DOC/DN, and N-acquiring enzyme activity (NAG + LAP) were significant predictors for NCF, and subsequent stepwise regression analysis retained temperature, fungal community composition, and NUE in the final model, with a negative effect of NUE on NCF. Gross N mineralization rates were positively related to gross nitrification (Fig. S7), which further indicates that NUE can affect the supply of NH_4^+-N to nitrifiers as well as NCF.

3.4. Structural equation model analyses

In surface soil, SEM analyses revealed that soil pH had a positive effect on NUE whereas DOC/DP had a negative effect on NUE (Fig. 4). Both N addition treatment and temperature indirectly influenced NUE through their effects on pH and DOC/DP. Total PLFA was positively affected by temperature and NUE and negatively affected by bacterial community composition in surface soil. NCF in surface soil was positively affected by temperature, bacterial community composition, and total PLFA, and negatively affected by NUE.

In subsurface soil, temperature had a positive effect on NUE and DOC/DN had a negative effect on total PLFA. NCF was positively affected by temperature and soil pH and negatively affected by NUE and fungal community composition. Temperature indirectly affected total PLFA by its effects on DOC/DN. N addition did not significantly affect NUE in subsurface soil (Fig. 4).

4. Discussion

4.1. Effects of N addition on microbial NUE in surface and subsurface soils

Nitrogen addition decreased microbial NUE in surface soil (Fig. 1), especially in the high N treatment. This effect was mainly driven by a decrease in microbial N growth rate but not by changes in gross N mineralization rate (Fig. S1). Microbial N growth rate and gross N mineralization rate did not change with N addition in subsurface soil, resulting in no obvious response of NUE to N addition in deeper soils. In contrast to our results, a previous study found that N addition increased microbial growth and NUE in the valley in a karst forest by increasing soil N availability (Yang et al., 2023). In the karst region, the underground conduit systems are well developed with hydrological processes dominated by vertical underground leakage (Fu et al., 2016), which is not conducive to soil nutrient retention. Therefore, karst ecosystems are usually limited by soil nutrients (Zhang et al., 2015). In contrast, we found that N addition decreased microbial growth and NUE by inducing soil acidification.

Consistent with previous studies (Sun et al., 2023a), microbial growth and NUE were positively related to soil pH (Fig. 2 and S5) in surface soil. This may be because microbial physiological responses to soil acidity increase maintenance costs to overcome H^+/Al^{3+} stress, lowering microbial growth rates (Fig. S5) and growth efficiency (including CUE and NUE) (Jones et al., 2019; Malik et al., 2018). However, Zhang et al. (2019) found no relationship between pH and microbial growth or NUE. These inconsistent results may be due to the indirect effect of pH on soil nutrient availability and microbial community composition (Schroeder et al., 2024; Zhang et al., 2019). The SEM results also indicated that N addition indirectly affected NUE by decreasing soil pH in surface soil (Fig. 4). Although soil pH also decreased with N addition in subsurface soil, the reduction was weaker than in surface soil (Fig. S1 and Fig. 4), and therefore was unrelated to NUE. These results are consistent with our first hypothesis.

4.2. Seasonal dynamics of microbial NUE in surface and subsurface soils

Microbial NUE was positively related to DP, and negatively related to DOC, DOC/DP, and DN/DP in surface soil (Fig. 2). This suggested that microbial metabolism was limited by P availability, consistent with the

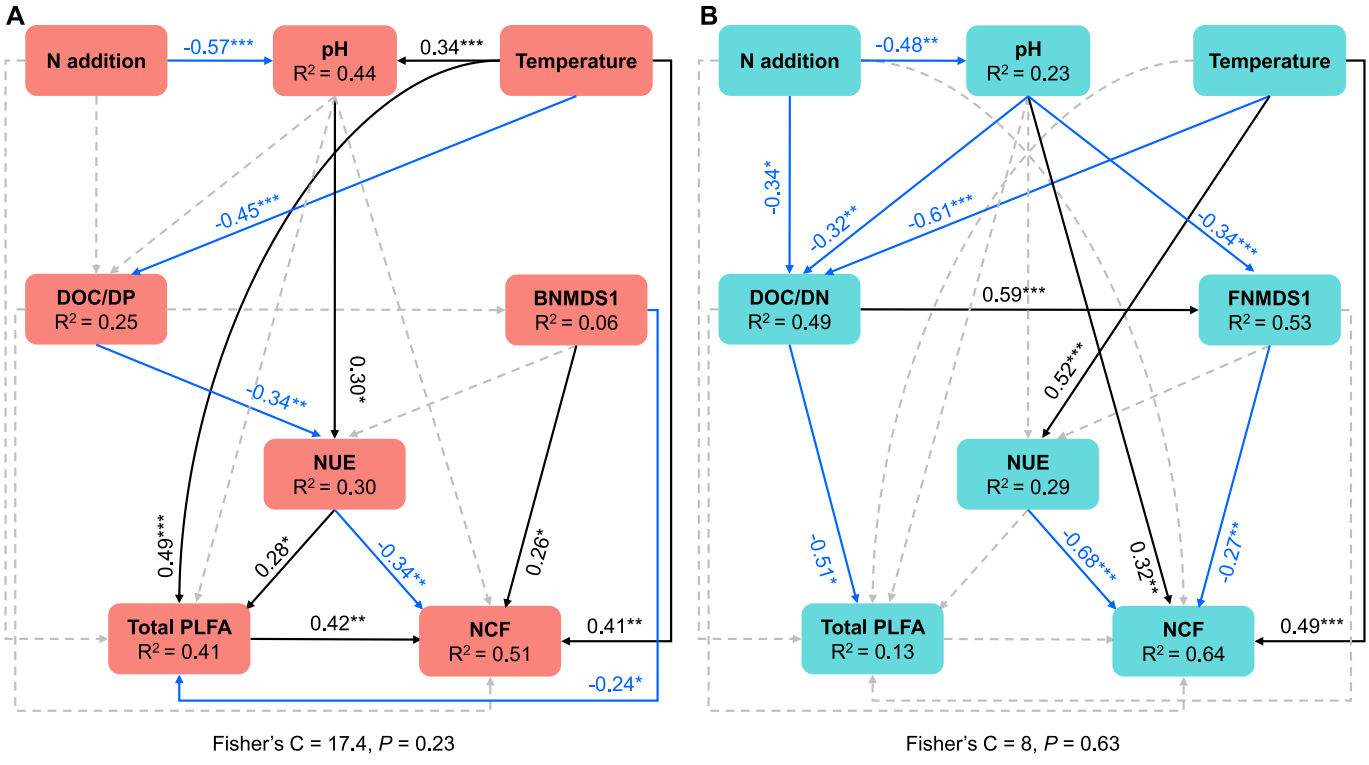

Fig. 4. Structural equation model describing the linkages among microbial NUE and measured variables in surface (A) and subsurface (B) soils. Numbers adjacent to arrows indicate standardized path coefficients and asterisks mark their significance: * , $P < 0.05$, ** , $P < 0.01$, *** , $P < 0.001$. Blue arrows indicate significant negative relationships, black arrows indicate significant positive relationships and gray arrows indicate pathways that are non-significant but improved the model-fit. Only significant path coefficients are shown, with the other non– significant path coefficients shown in Table S3. The test statistic of Fisher's C and *P* values in surface soil were 17.4 and 0.23, respectively, and in subsurface soil they are 8 and 0.63, respectively. DOC/DP, the ratio of dissolved organic carbon to dissolved phosphorus; DOC/DN, the ratio of dissolved organic carbon to dissolved nitrogen; PLFA, phospholipid fatty acids (nmol g^{-1}); NCF, composite inorganic nitrogen cycling flux (ng g^{-1} h^{-1}); BNMDS1, bacterial community non-metric multidimensional scaling (NMDS) axis 1; FNMDS1, fungal community non-metric multidimensional scaling (NMDS) axis 1.

negative relationship between NUE and P-acquiring enzyme activity (AP) but not to C-acquiring (BG) and N-acquiring enzyme activities (NAG + LAP). Under P limiting conditions microbial growth (and therefore NUE) is reduced and microbes tend to increase resource investment in AP production rather than growth, which may further decrease NUE. Some studies have argued that microbes are generally limited by C in soils, such that NUE would increase with C availability if N becomes relatively more constrained in parallel (Feng et al., 2022; Sun et al., 2023a; Zhang et al., 2019). However, we found a negative relationship between C availability and microbial NUE (Fig. 2), suggesting that other (limiting) factors covary with C availability and it is those "hidden" factors that actually limit microbial growth and reduce NUE. This hints at the broader importance of substrate stoichiometries and eventually P limiting microbial growth efficiency (Manzoni et al., 2012; Prommer et al., 2020; Tian et al., 2023). Previous studies found continuous N addition induced P limitation of microbial metabolism in tropical forests with low P availability (Deng et al., 2017). Our results indicate that this phenomenon also exists in temperate forests which are typically characterized as N-limited ecosystems (Reich et al., 1997). Yuan et al. (2024) previously showed that N addition stimulated tree growth in the temperate forest in the current study, which may further decrease P availability for soil microbes by increasing plant P uptake. In subsurface soil, the effect of P limitation on microbial metabolism was not observed under N addition, possibly due to less impact on pH in subsurface.

Towards summer, i.e. with increasing soil temperature, microbial NUE was stimulated indirectly in surface soil, following increases in soil pH and decreasing DOC/DP. In contrast, a direct positive effect of soil temperature on NUE was observed in subsurface soil (Fig. 4), consistent with our second hypothesis. By way of explanation, a large amount of litterfall in the study area occurs between late September and early October (Li et al., 2015). During autumn season soil temperatures were lowest (7 °C in October) at the study site, but soil dissolved organic carbon content was highest, likely due to increased litter inputs (Fig. S2). At the same time soil pH decreased, also possibly due to the litter inputs (Fig. S1) (Dai et al., 2021). Such seasonal changes in litter input can result in an apparent positive relationship between soil temperature and soil pH and a negative association to DOC/DP in surface soils, with corresponding changes in microbial NUE (Fig. 4). Thus, in contrast to the direct effect of temperature on NUE in subsurface soil, the indirect effects of temperature on NUE in surface soil may reflect climate-plant-soil interactions on microbial metabolism under N addition (Li et al., 2023). These interaction effects would decrease with soil depth.

4.3. Relationships between microbial NUE and microbial biomass

In partial agreement with our third hypothesis, microbial NUE was positively related to microbial biomass (total PLFA, fungal PLFA, bacterial PLFA, and G^+ and G^- PLFA) in the surface but not in subsurface soil (Fig. 2 and Table S2). A high NUE resulted from high microbial growth and biomass synthesis in the surface soil. However, microbial biomass in subsurface soil was mainly affected by N substrate availability rather than NUE (Figs. 3 and 4), likely because substrate availability typically decreases with depth (Liu et al., 2023). This was likely due to the lower substrate content and stronger physical protection (higher clay and silt contents and higher mineral-associated organic matter) in the subsurface than surface soil (Table 1 and Fig. S3) (Xu and Tsang, 2024). These results suggest that the relationship between microbial growth efficiency and biomass production is regulated by other factors (such as substrate availability and soil pH) (Malik et al., 2018; Sun et al., 2021), providing an alternative perspective to increases in soil C storage with N addition. Previous studies found that increased microbial CUE promoted soil C conservation by stimulating the production of microbial biomass and subsequent accumulation of microbial residues (Liang et al., 2017; Tao et al., 2023). We suspect that this stimulation of soil C storage may also be enhanced by higher NUE. The global average of microbial biomass C:N stoichiometry is about 7 (Xu et al., 2013), which implies that an increase in microbial biomass N related to an increasing NUE would lead to a seven-fold increase in microbial biomass C. Therefore, the potential and positive effects of microbial NUE on soil C storage seem worth studying.

We further found that the stimulation of microbial NUE under N addition was paralleled by a stronger N amendment effect for fungi than for bacteria, resulting in a positive relationship between NUE and the ratio of fungi:bacteria in surface soil (Fig. 2 and S6), consistent with the strong negative effect of N addition on both fungal PLFA and NUE (Fig. S5 and 1). A global *meta*-analysis also showed a significant decrease in fungal PLFA but not bacterial PLFA with N addition rate (Zhang et al., 2018). High N availability may inhibit fungal proliferation and reduce fungal biomass via changes in nutrient competition between plants and rhizosphere microbes, by changes in plant-specific exudates or via inducing the production of compounds that are toxic to fungi (Treseder, 2008; Zhang et al., 2018). An alternative explanation may be that fungal abundance was significantly lower than bacteria (Fig. S6) with fungal biomass being more prone to change and showing a stronger correlation with microbial NUE. Regardless, our results were in contrast to previous theory predicting that NUE should be negatively related to the fungi: bacterias ratio because fungi have a lower N demand than bacteria (Mooshammer et al., 2014b). However, recent studies found that growth rate and growth efficiency varied greatly within and among microbial taxa (Pold et al., 2020). In the future, new methods (such as quantitative stable isotope probing techniques) exploring active microbial taxa and their individual growth rates and growth efficiencies may help to understand these contradictory results.

4.4. Relationships between microbial NUE and soil inorganic N cycling

We here provide solid evidence that microbial NUE was negatively related to soil inorganic N cycling fluxes (Table S2 and Figs. 3 and 4), consistent with our third hypothesis. In natural systems, soil inorganic N supply depends largely on organic N mineralization (Li et al., 2020), which is inversely related to microbial NUE (Fig. S4). The inorganic N produced by gross N mineralization i.e. NH_4^+-N can stimulate NO_3^--N production through nitrification (Fig. S7) and subsequent consumption processes of NH_4^+-N and NO_3^--N through inorganic N cycling (Sun et al., 2021; Sun et al., 2019; Zhang et al., 2013; Zhang et al., 2012; Zhang et al., 2019), affecting the entire balance of soil inorganic N cycling. Previous studies have mostly focussed on specific N transformation processes and their relationships to microbial NUE (Zhang et al., 2019), with few studies focused on the entire soil inorganic N cycle. Our results suggest that microbial NUE is a key index to soil inorganic N cycling. However, it should be noted that soil sieving disrupted any mycelial networks in this forest soil, so that the N transformation rates estimated in this study may have been altered by the turnover of fungal mycelia and do not reflect field conditions (Gao et al., 2016). In-situ experiments are needed to better understand the effects of NUE on soil N cycling under field conditions.

5. Conclusions

The effects of N addition on microbial NUE depended on soil depth, season, and rate of N addition. In surface soil, high N addition acidified the soil, inhibited microbial growth and reduced NUE. However, N addition did not affect NUE in subsurface soil, possibly due to the buffering effects of the overlying surface soil. Microbial NUE in surface soil was also limited by P, suggesting that long-term N addition may have induced a P limitation for microbial metabolism. Microbial NUE in the subsurface soil was mainly regulated by temperature. These results imply a stronger climate-plant-soil interaction on microbial metabolism in surface than subsurface soil under N addition, mediated by the seasonality of litter inputs affecting both soil pH and DOC pools. We further

found NUE to be inversely related to microbial biomass production and soil inorganic N cycling, demonstrating a central position of microbial NUE in the flux of organic N to inorganic N. Therefore, NUE is strongly related to soil N cycling and so biogeochemical models should incorporate variable NUE to better predict soil N dynamics in future climates.

CRediT authorship contribution statement

Lifei Sun: Writing – original draft, Visualization, Funding acquisition, Formal analysis, Conceptualization. **Yanci Qiao:** Software, Formal analysis. **Wolfgang Wanek:** Writing – review & editing, Formal analysis, Conceptualization. **Daryl L. Moorhead:** Writing – review & editing, Visualization, Formal analysis. **Yongxing Cui:** Writing – review & editing, Formal analysis. **Yujiao Peng:** Formal analysis. **Liquan Song:** Writing – original draft, Formal analysis. **Baoqing Hu:** Writing – review & editing, Funding acquisition, Formal analysis. **Tuo Zhang:** Writing – review & editing, Formal analysis. **Shuailin Li:** Writing – review & editing, Formal analysis.

Declaration of competing interest

The authors declare that they have no known competing financial interests or personal relationships that could have appeared to influence the work reported in this paper.

Acknowledgments

This work was funded by the Key Research and Development Program of China (2020YFA0608100), National Natural Science Foundation of China (32001174, 42071135, 42271135), The Opening Foundation of Key Laboratory of Environment Change and Resources Use in Beibu Gulf, Ministry of Education, Nanning Normal University (NO.NNNU-KLOP-X2401), and Project funded by China Postdoctoral Science Foundation (2022M710004).

Appendix A. Supplementary data

Supplementary data to this article can be found online at https://doi.org/10.1016/j.geoderma.2024.117159.

Data availability

Data will be made available on request.

References

Allison, S.D., LeBauer, D.S., Ofrecio, M.R., Reyes, R., Ta, A.-M., Tran, T.M., 2009. Low levels of nitrogen addition stimulate decomposition by boreal forest fungi. Soil Biol. Biochem. 41 (2), 293–302.
Archer, E., 2016. rfPermute: estimate permutation p-values for random forest importance metrics. R Package Version 1 (2).
Bai, E., Li, W., Li, S., Sun, J., Peng, B., Dai, W., Jiang, P., Han, S., 2014. Pulse increase of soil N2O emission in response to N addition in a temperate forest on Mt Changbai, northeast China. PLoS One 9 (7), e102765.
Brookes, P.C., Powlson, D.S., Jenkinson, D.S., 1982. Measurement of microbial biomass phosphorus in soil. Soil Biol. Biochem. 14 (4), 319–329.
Brooks, P., Stark, J.M., McInteer, B., Preston, T., 1989. Diffusion method to prepare soil extracts for automated nitrogen-15 analysis. Soil Sci. Soc. Am. J. 53 (6), 1707–1711.
Cui, Y., Moorhead, D.L., Guo, X., Peng, S., Wang, Y., Zhang, X., Fang, L., 2021. Stoichiometric models of microbial metabolic limitation in soil systems. Global Ecol. Biogeogr. 30 (11), 2297–2311.
Dai, W., Peng, B., Liu, J., Wang, C., Wang, X., Jiang, P., Bai, E., 2021. Four years of litter input manipulation changes soil microbial characteristics in a temperate mixed forest. Biogeochemistry 154 (2), 371–383.
Davidson, E.A., Hart, S.C., Shanks, C.A., Firestone, M.K., 1991. Measuring gross nitrogen mineralization, and nitrification by ^{15}N isotopic pool dilution in intact soil cores. J. Soil Sci. 42 (3), 335–349.
Deng, Q., Hui, D., Dennis, S., Reddy, K.C., 2017. Responses of terrestrial ecosystem phosphorus cycling to nitrogen addition: a meta-analysis. Global Ecol. Biogeogr. 26 (6), 713–728.
Dentener, F., Drevet, J., Lamarque, J.F., Bey, I., Eickhout, B., Fiore, A.M., Hauglustaine, D., Horowitz, L.W., Krol, M., Kulshrestha, U.C., Lawrence, M., Galy-Lacaux, C., Rast, S., Shindell, D., Stevenson, D., Van Noije, T., Atherton, C., Bell, N., Bergman, D., Butler, T., Cofala, J., Collins, B., Doherty, R., Ellingsen, K., Galloway, J., Gauss, M., Montanaro, V., Müller, J.F., Pitari, G., Rodriguez, J., Sanderson, M., Solmon, F., Strahan, S., Schultz, M., Sudo, K., Szopa, S., Wild, O., 2006. Nitrogen and sulfur deposition on regional and global scales: a multimodel evaluation. Global Biogeochem. Cycles 20 (4).
Domeignoz-Horta, L.A., Pold, G., Liu, X.-J.-A., Frey, S.D., Melillo, J.M., DeAngelis, K.M., 2020. Microbial diversity drives carbon use efficiency in a model soil. Nat. Commun. 11 (1), 3684.
Elrys, A.S., Ali, A., Zhang, H., Cheng, Y., Zhang, J., Cai, Z.-C., Müller, C., Chang, S.X., 2021a. Patterns and drivers of global gross nitrogen mineralization in soils. Global Change Biol. 27 (22), 5950–5962.
Elrys, A.S., Wang, J., Metwally, M.A.S., Cheng, Y., Zhang, J.-B., Cai, Z.-C., Chang, S.X., Müller, C., 2021b. Global gross nitrification rates are dominantly driven by soil carbon-to-nitrogen stoichiometry and total nitrogen. Global Change Biol. 27 (24), 6512–6524.
Feng, X., Qin, S., Zhang, D., Chen, P., Hu, J., Wang, G., Liu, Y., Wei, B., Li, Q., Yang, Y., Chen, L., 2022. Nitrogen input enhances microbial carbon use efficiency by altering plant–microbe–mineral interactions. Global Change Biol. 28 (16), 4845–4860.
Francisco, R., Duarte, T., Chelinho, S., Maleita, C.M.N., Braga, M.E.M., Cunha, M.J., Abrantes, I., de Sousa, H.C., Sousa, J.P., Morais, P.V., 2022. Effects of a bionematicide 1,4-naphthoquinone solution on soil microbial community assessed by PLFA: Tracing toxicity indicators. Appl. Soil Ecol. 174, 104417.
Frostegård, Å., Bååth, E., Tunlio, A., 1993. Shifts in the structure of soil microbial communities in limed forests as revealed by phospholipid fatty acid analysis. Soil Biol. Biochem. 25 (6), 723–730.
Fu, Z., Chen, H., Xu, Q., Jia, J., Wang, S., Wang, K., 2016. Role of epikarst in near-surface hydrological processes in a soil mantled subtropical dolomite karst slope: implications of field rainfall simulation experiments. Hydrol. Process. 30 (5), 795–811.
Galloway, J.N., Townsend, A.R., Erisman, J.W., Bekunda, M., Cai, Z., Freney, J.R., Martinelli, L.A., Seitzinger, S.P., Sutton, M.A., 2008. Transformation of the nitrogen cycle: recent trends, questions, and potential solutions. Science 320 (5878), 889.
Gao, W., Kou, L., Zhang, J., Müller, C., Wang, H., Yang, H., Li, S., 2016. Enhanced deposition of nitrate alters microbial cycling of N in a subtropical forest soil. Biol. Fert. Soils 52 (7), 977–986.
Gee, G.W., Bauder, J.W., 1986. Particle-size Analysis, Methods of soil analysis: Part 1 Physical and mineralogical methods, 5 (1986). SSSA Book Series 383–411.
German, D.P., Weintraub, M.N., Grandy, A.S., Lauber, C.L., Rinkes, Z.L., Allison, S.D., 2011. Optimization of hydrolytic and oxidative enzyme methods for ecosystem studies. Soil Biol. Biochem. 43 (7), 1387–1397.
Huygens, D., Boeckx, P., Templer, P., Paulino, L., Van Cleemput, O., Oyarzún, C., Müller, C., Godoy, R., 2008. Mechanisms for retention of bioavailable nitrogen in volcanic rainforest soils. Nat. Geosci. 1 (8), 543–548.
Jan, M.T., Roberts, P., Tonheim, S.K., Jones, D.L., 2009. Protein breakdown represents a major bottleneck in nitrogen cycling in grassland soils. Soil Biol. Biochem. 41 (11), 2272–2282.
Jones, D.L., Cooledge, E.C., Hoyle, F.C., Griffiths, R.I., Murphy, D.V., 2019. pH and exchangeable aluminum are major regulators of microbial energy flow and carbon use efficiency in soil microbial communities. Soil Biol. Biochem. 138, 107584.
Kirkham, D., Bartholomew, W.V., 1954. Equations for following nutrient transformations in soil, utilizing tracer data. Soil Sci. Soc. Am. J. 18 (1), 33–34.
Lefcheck, J.S., 2016. piecewiseSEM: Piecewise structural equation modelling in r for ecology, evolution, and systematics. Methods Ecol. Evol. 7 (5), 573–579.
Lever, M.A., Rogers, K.L., Lloyd, K.G., Overmann, J., Schink, B., Thauer, R.K., Hoehler, T. M., Jørgensen, B.B., 2015. Life under extreme energy limitation: a synthesis of laboratory- and field-based investigations. FEMS Microbiol. Rev. 39 (5), 688–728.
Li, J., Sang, C., Yang, J., Qu, L., Xia, Z., Sun, H., Jiang, P., Wang, X., He, H., Wang, C., 2021. Stoichiometric imbalance and microbial community regulate microbial elements use efficiencies under nitrogen addition. Soil Biol. Biochem. 156, 108207.
Li, X., Yin, X., Wang, Z., Fan, W., 2015. Litter mass loss and nutrient release influenced by soil fauna of Betula ermanii forest floor of the Changbai Mountains, China. Appl. Soil Ecol. 95, 15–22.
Li, Z., Zeng, Z., Tian, D., Wang, J., Wang, B., Chen, H.Y.H., Quan, Q., Chen, W., Yang, J., Meng, C., Wang, Y., Niu, S., 2020. Global variations and controlling factors of soil nitrogen turnover rate. Earth-Sci. Rev. 207, 103250.
Li, F., Zi, H., Sonne, C., Li, X., 2023. Microbiome sustains forest ecosystem functions across hierarchical scales. Eco-Environ. Health 2 (1), 24–31.
Liang, C., Schimel, J.P., Jastrow, J.D., 2017. The importance of anabolism in microbial control over soil carbon storage. Nat. Microbiol. 2 (8), 17105.
Liu, J., Peng, B., Xia, Z., Sun, J., Gao, D., Dai, W., Jiang, P., Bai, E., 2017. Different fates of deposited NH_4^+ and NO_3^- in a temperate forest in northeast China: a ^{15}N tracer study. Global Change Biol. 23 (6), 2441–2449.
Liu, Y., Zou, X., Chen, H.Y.H., Delgado-Baquerizo, M., Wang, C., Zhang, C., Ruan, H., 2023. Fungal necromass is reduced by intensive drought in subsoil but not in topsoil. Global Change Biol. n/a(n/a).
Malik, A.A., Puissant, J., Buckeridge, K.M., Goodall, T., Jehmlich, N., Chowdhury, S., Gweon, H.S., Peyton, J.M., Mason, K.E., van Agtmaal, M., Blaud, A., Clark, I.M., Whitaker, J., Pywell, R.F., Ostle, N., Gleixner, G., Griffiths, R.I., 2018. Land use driven change in soil pH affects microbial carbon cycling processes. Nat. Commun. 9 (1), 3591.
Manzoni, S., Taylor, P., Richter, A., Porporato, A., Ågren, G.I., 2012. Environmental and stoichiometric controls on microbial carbon-use efficiency in soils. New Phytol. 196 (1), 79–91.
Mooshammer, M., Wanek, W., Hämmerle, I., Fuchslueger, L., Hofhansl, F., Knoltsch, A., Schnecker, J., Takriti, M., Watzka, M., Wild, B., Keiblinger, K.M., Zechmeister-

Boltenstern, S., Richter, A., 2014a. Adjustment of microbial nitrogen use efficiency to carbon:nitrogen imbalances regulates soil nitrogen cycling. Nat. Commun. 5 (1), 3694.
Mooshammer, M., Wanek, W., Zechmeister-Boltenstern, S., Richter, A., 2014b. Stoichiometric imbalances between terrestrial decomposer communities and their resources: mechanisms and implications of microbial adaptations to their resources. Front. Microbiol. 5 (22), 22.
Müller, C., Rütting, T., Kattge, J., Laughlin, R.J., Stevens, R.J., 2007. Estimation of parameters in complex ^{15}N tracing models by Monte Carlo sampling. Soil Biol. Biochem. 39 (3), 715–726.
Olsson, P.A., Thingstrup, I., Jakobsen, I., Bååth, E., 1999. Estimation of the biomass of arbuscular mycorrhizal fungi in a linseed field. Soil Biol. Biochem. 31 (13), 1879–1887.
Pinheiro, J., 2011. nlme: Linear and nonlinear mixed effects models. R Package Version 3, 1.
Poeplau, C., Don, A., Six, J., Kaiser, M., Benbi, D., Chenu, C., Cotrufo, M.F., Derrien, D., Gioacchini, P., Grand, S., Gregorich, E., Griepentrog, M., Gunina, A., Haddix, M., Kuzyakov, Y., Kühnel, A., Macdonald, L.M., Soong, J., Trigalet, S., Vermeire, M.-L., Rovira, P., van Wesemael, B., Wiesmeier, M., Yeasmin, S., Yevdokimov, I., Nieder, R., 2018. Isolating organic carbon fractions with varying turnover rates in temperate agricultural soils – A comprehensive method comparison. Soil Biol. Biochem. 125, 10–26.
Pold, G., Domeignoz-Horta, L.A., Morrison, E.W., Frey, S.D., Sistla, S.A., DeAngelis, K.M., 2020. Carbon use efficiency and its temperature sensitivity covary in soil Bacteria. MBio 11 (1) e02293-02219.
Prommer, J., Walker, T.W.N., Wanek, W., Braun, J., Zezula, D., Hu, Y., Hofhansl, F., Richter, A., 2020. Increased microbial growth, biomass, and turnover drive soil organic carbon accumulation at higher plant diversity. Global Change Biol. 26 (2), 669–681.
Reich, P.B., Grigal, D.F., Aber, J.D., Gower, S.T., 1997. Nitrogen mineralization and productivity in 50 hardwood and conifer stands on diverse soils. Ecology 78 (2), 335–347.
Saiya-Cork, K.R., Sinsabaugh, R.L., Zak, D.R., 2002. The effects of long term nitrogen deposition on extracellular enzyme activity in an Acer saccharum forest soil. Soil Biol. Biochem. 34 (9), 1309–1315.
Sang, C., Xia, Z., Sun, L., Sun, H., Jiang, P., Wang, C., Bai, E., 2021. Responses of soil microbial communities to freeze–thaw cycles in a Chinese temperate forest. Ecol. Process. 10 (1), 66.
Schimel, J.P., Bennett, J., 2004. Nitrogen mineralization: challenges of a changing paradigm. Ecology 85 (3), 591–602.
Schroeder, J., Dămătîrcă, C., Bölscher, T., Chenu, C., Elsgaard, L., Tebbe, C.C., Skadell, L., Poeplau, C., 2024. Liming effects on microbial carbon use efficiency and its potential consequences for soil organic carbon stocks. Soil Biol. Biochem. 191, 109342.
Shipley, B., 2013. The AIC model selection method applied to path analytic models compared using a d-separation test. Ecology 94 (3), 560–564.
Spohn, M., Klaus, K., Wanek, W., Richter, A., 2016. Microbial carbon use efficiency and biomass turnover times depending on soil depth-Implications for carbon cycling. Soil Biol. Biochem. 96, 74–81.
Sun, L., Xia, Z., Sang, C., Wang, X., Peng, B., Wang, C., Zhang, J., Müller, C., Bai, E., 2019. Soil resource status affects the responses of nitrogen processes to changes in temperature and moisture. Biol. Fert. Soils 55 (6), 629–641.
Sun, L., Wang, C., Yu, H., Liu, D., Houlton, B.Z., Wang, S., Zeng, X., Bai, E., Fang, Y., Jia, Y., 2021. Biotic and abiotic controls on dinitrogen production in coastal sediments. Global Biogeochem. Cycles 35 (12) e2021GB007069.
Sun, L., Li, J., Qu, L., Wang, X., Sang, C., Wang, J., Sun, M., Wanek, W., Moorhead, D.L., Bai, E., Wang, C., 2023a. Phosphorus limitation reduces microbial nitrogen use efficiency by increasing extracellular enzyme investments. Geoderma 432, 116416.
Sun, L., Moorhead, D.L., Cui, Y., Wanek, W., Li, S., Wang, C., 2023b. Exogenous nitrogen input skews estimates of microbial nitrogen use efficiency by ecoenzymatic stoichiometry. Ecol. Process. 12 (1), 46.
Tao, F., Huang, Y., Hungate, B.A., Manzoni, S., Frey, S.D., Schmidt, M.W.I., Reichstein, M., Carvalhais, N., Ciais, P., Jiang, L., Lehmann, J., Wang, Y.-P., Houlton, B.Z., Ahrens, B., Mishra, U., Hugelius, G., Hocking, T.D., Lu, X., Shi, Z., Viatkin, K., Vargas, R., Yigini, Y., Omuto, C., Malik, A.A., Peralta, G., Cuevas-Corona, R., Di Paolo, L.E., Luotto, I., Liao, C., Liang, Y.-S., Saynes, V.S., Huang, X., Luo, Y., 2023. Microbial carbon use efficiency promotes global soil carbon storage. Nature 618 (7967), 981–985.
Tian, Y., Schindlbacher, A., Malo, C.U., Shi, C., Heinzle, J., Kwatcho Kengdo, S., Inselsbacher, E., Borken, W., Wanek, W., 2023. Long-term warming of a forest soil reduces microbial biomass and its carbon and nitrogen use efficiencies. Soil Biol. Biochem. 184, 109109.
Treseder, K.K., 2008. Nitrogen additions and microbial biomass: a meta-analysis of ecosystem studies. Ecol. Lett. 11 (10), 1111–1120.
Valero-Mora, P.M., 2010. ggplot2: elegant graphics for data analysis. J. Stat. Softw. 35, 1–3.
Vance, E.D., Brookes, P.C., Jenkinson, D.S., 1987. An extraction method for measuring soil microbial biomass C. Soil Biol. Biochem. 19 (6), 703–707.
Wang, Q., Wang, S., He, T., Liu, L., Wu, J., 2014. Response of organic carbon mineralization and microbial community to leaf litter and nutrient additions in subtropical forest soils. Soil Biol. Biochem. 71, 13–20.
Wei, T., Simko, V., Levy, M., Xie, Y., Jin, Y., Zemla, J., 2017. Package 'corrplot'. Statistician 56 (316), e24.
Xu, X., Thornton, P.E., Post, W.M., 2013. A global analysis of soil microbial biomass carbon, nitrogen and phosphorus in terrestrial ecosystems. Global Ecol. Biogeogr. 22 (6), 737–749.
Xu, Z., Tsang, D.C.W., 2024. Mineral-mediated stability of organic carbon in soil and relevant interaction mechanisms. Eco-Environ. Health 3 (1), 59–76.
Yang, X., Duan, P., Hicks, L., Wang, K., Li, D., 2023. Mechanisms underlying the responses of microbial carbon and nitrogen use efficiencies to nitrogen addition are mediated by topography in a subtropical forest. Sci. Total Environ. 880, 163236.
Yang, Y., Xie, H., Mao, Z., Bao, X., He, H., Zhang, X., Liang, C., 2022. Fungi determine increased soil organic carbon more than bacteria through their necromass inputs in conservation tillage croplands. Soil Biol. Biochem. 167, 108587.
Yu, G., Jia, Y., He, N., Zhu, J., Chen, Z., Wang, Q., Piao, S., Liu, X., He, H., Guo, X., Wen, Z., Li, P., Ding, G., Goulding, K., 2019. Stabilization of atmospheric nitrogen deposition in China over the past decade. Nat. Geosci. 12 (6), 424–429.
Yuan, Z., Osei, R., Mao, Z., Ye, J., Lin, F., Fang, S., Wang, X., Hao, Z., Ali, A., 2024. Determinants of tree population temporal stability in a temperate mixed forest over a gradient of nitrogen addition. J. Environ. Manage. 368, 122198.
Zhang, T.A., Chen, H.Y.H., Ruan, H., 2018. Global negative effects of nitrogen deposition on soil microbes. ISME. J. 12 (7), 1817–1825.
Zhang, W., Zhao, J., Pan, F., Li, D., Chen, H., Wang, K., 2015. Changes in nitrogen and phosphorus limitation during secondary succession in a karst region in southwest China. Plant Soil 391 (1), 77–91.
Zhang, S., Zheng, Q., Noll, L., Hu, Y., Wanek, W., 2019. Environmental effects on soil microbial nitrogen use efficiency are controlled by allocation of organic nitrogen to microbial growth and regulate gross N mineralization. Soil Biol. Biochem. 135, 304–315.
Zhang, J., Zhu, T., Cai, Z., Müller, C., 2011. Nitrogen cycling in forest soils across climate gradients in Eastern China. Plant Soil 342 (1–2), 419–432.
Zhang, J.B., Zhu, T.B., Cai, Z.C., Qin, S.W., Müller, C., 2012. Effects of long-term repeated mineral and organic fertilizer applications on soil nitrogen transformations. Eur. J. Soil Sci. 63 (1), 75–85.
Zhang, J., Zhu, T., Meng, T., Zhang, Y., Yang, J., Yang, W., Müller, C., Cai, Z., 2013. Agricultural land use affects nitrate production and conservation in humid subtropical soils in China. Soil Biol. Biochem. 62, 107–114.
Zhu, X., Zhang, W., Chen, H., Mo, J., 2015. Impacts of nitrogen deposition on soil nitrogen cycle in forest ecosystems: a review. Acta Ecol. Sin. 35 (3), 35–43.